

Florida State University Libraries

2016-12

An Efficient And Long-time Accurate Third-order Algorithm For The Stokes-darcy System

Wenbin Chen, Max Gunzburger, Dong Sun and Xiaoming Wang

The publisher's version of record is available at <https://doi.org/10.1007/s00211-015-0789-3>



An efficient and Long-Time Accurate Third-Order Algorithm for the Stokes-Darcy System

Wenbin Chen · Max Gunzburger · Dong Sun · Xiaoming Wang

Received: date / Accepted: date

Abstract A third-order in time numerical IMEX-type algorithm for the Stokes-Darcy system for flows in fluid saturated karst aquifers is proposed and analyzed. A novel third-order Adams-Moulton scheme is used for the discretization of the dissipative term whereas a third-order explicit Adams-Bashforth scheme is used for the time discretization of the interface term that couples the Stokes and Darcy components. The scheme is efficient in the sense that one needs to solve, at each time step, decoupled Stokes and Darcy problems. Therefore, legacy Stokes and Darcy solvers can be applied in parallel. The scheme is also unconditionally stable and, with a mild time-step restriction, long-time accurate in the sense that the error is bounded uniformly in time. Numerical experiments are used to illustrate the theoretical results. To the authors' knowledge, the novel algorithm is the first third-order accurate numerical scheme for the Stokes-Darcy system possessing its favorable efficiency, stability, and accuracy properties.

This work is supported in part by a grant from the NSF.

Wenbin Chen
School of Mathematical Sciences, Fudan University
E-mail: wbchen@fudan.edu.cn

Max Gunzburger
Department of Scientific Computing, Florida State University
E-mail: gunzburg@fsu.edu

Dong Sun
Department of Mathematics, Florida State University
E-mail: dsun@math.fsu.edu

Xiaoming Wang
Department of Mathematics, Florida State University
E-mail: wxm@math.fsu.edu *Corresponding author*

Keywords Stokes-Darcy system · Adams-Moulton-Bashforth method · unconditional stability · uniform in time error estimates · third-order accurate in time · karst aquifers

Mathematics Subject Classification (2000) 35M13 · 35Q35 · 65N30 · 65N55 · 76D07 · 76S05

1 Introduction

Certain rocks such as limestone, dolomite and gypsum are susceptible to dissolution due to reaction with carbon-dioxide and water which leads, over long (geological) time, to the formation of voids (vugs) and conduits. This type of landscape is referred to as karst. Due to the existence of vugs and conduits, large amount of water may be stored in karst regions to form karst aquifers that are of great practical importance and are susceptible to pollution [34]. For example, about 90% of the fresh water used in the State of Florida comes from karst aquifers and contamination is a serious problem [32].

For many important applications such as contaminant transport in karst aquifers, one must couple the fluid motion in the porous media with the fluid motion in the conduit or vugs. For instance, contaminants driven into the porous media during a flood season may be released during a drought season. Moreover, because fluid motion in the porous media (matrix) is much slower compared to fluid motion in conduits, long-time accurate numerical schemes are highly desirable if one is interested in capturing the physically interesting retention and release of contaminants within karst aquifers.

There has been a recent surge in interest in the design and analysis of numerical algorithms for the Stokes-Darcy and related systems that govern the motion of fluids flows in saturated karst aquifers. See, e.g., [9–11, 14–16, 19–23, 25, 33, 35–42, 45–48]. In particular, first order and second order in time accurate and long-time stable schemes have been proposed and studied in [11, 16, 36, 37, 42].

The purpose of this work is to propose and investigate a novel third-order Adams-Moulton-Bashforth method for the Stokes-Darcy system. The algorithm is a special case of the implicit-explicit (IMEX) class of schemes [1–3, 5]. The coupling term in the interface conditions is treated explicitly in our algorithm so that only two decoupled problems (one Stokes and one Darcy) are solved at each time step. Therefore, the scheme can be implemented very efficiently and, in particular, legacy codes for each of the two components can be utilized. Moreover, we show that our scheme is unconditionally stable and long-time stable in the sense that the solutions remain bounded uniformly in time. The uniform in time bound of the solutions further leads to uniform in time error estimates. This is a highly desirable feature because one would want to have reliable numerical results over the long-time scale of contaminant sequestration and release. We also provide the results of numerical experiments that illustrate our analytical results.

38 This work can be viewed as an improvement of our earlier work [16] in
 39 which a second-order in time Adams-Moulton-Bashforth algorithm was stud-
 40 ied. This is the first third-order algorithm that is unconditionally stable, long-
 41 time accurate in the sense of the existence of a uniform-in-time error bound,
 42 and efficient in the sense that only two decoupled problems (one Stokes, one
 43 Darcy) are needed at each time step.

44 The rest of the paper is organized as follows. In Section 2, we introduce the
 45 coupled Stokes-Darcy system, the associated weak formulation, and the third-
 46 order in time scheme. The unconditional and long-time stability with respect
 47 to the L^2 norm are presented in Section 3. Numerical results that illustrate
 48 the accuracy, efficiency, and long-time stability of our algorithms are given in
 49 Section 4. We close by providing some concluding remarks in Section 5.

50 2 The Stokes-Darcy system and one type of third order IMEX 51 method

52 In this section we recall the Stokes-Darcy system modeling flows in saturated
 53 karst aquifers. A third-order in time numerical scheme based on the Adams-
 54 Moulton-Bashforth approach is presented as well.

55 *The Stokes-Darcy system.* For simplicity, the following conceptual domain is
 56 considered for a karst aquifer. It contains a porous media (matrix), denoted
 57 by $\Omega_p \in \mathbb{R}^d$, and a conduit, denoted by $\Omega_f \in \mathbb{R}^d$, where $d = 2, 3$ denotes the
 58 spatial dimension. Γ denotes the interface between the matrix and the conduit.
 59 The remaining pieces of the boundaries for the matrix and the conduit are
 60 denoted $\partial\Omega_p$ and $\partial\Omega_f$, respectively. We assume $\partial\Omega_p$ and $\partial\Omega_f$ are non-empty
 61 for simplicity.

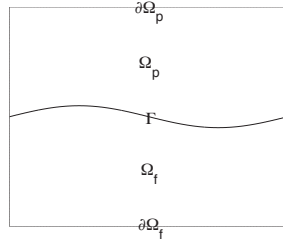


Fig. 1 The physical domain consisting of a porous media Ω_p and a free-flow conduit Ω_f .

The governing coupled Stokes-Darcy system for karst aquifers is given by

$$\begin{cases} S \frac{\partial \phi}{\partial t} - \nabla \cdot (\mathbb{K} \nabla \phi) = f & \text{in } \Omega_p, \\ \frac{\partial \mathbf{u}_f}{\partial t} - \frac{1}{\rho} \nabla \cdot \mathbb{T}(\mathbf{u}_f, p) = \mathbf{f} \quad \text{and} \quad \nabla \cdot \mathbf{u}_f = 0 & \text{in } \Omega_f, \end{cases} \quad (1)$$

where the unknowns are the hydraulic head ϕ in the matrix and the fluid velocity \mathbf{u}_f and the pressure p in the conduit [18]. The Darcy velocity \mathbf{u}_p in the matrix can be recovered by the Darcy equation $\mathbf{u}_p = -\mathbb{K}\nabla\phi$. In (1), f denotes a sink or source in the matrix, \mathbf{f} denotes a body force density in the conduit, ρ the fluid density which is taken to be 1 for simplicity, $\mathbb{T}(\mathbf{u}_f, p) = 2\nu\mathbb{D}(\mathbf{u}_f) - p\mathbb{I}$ denotes the stress tensor in the conduit, and $\mathbb{D}(\mathbf{u}_f) = (\nabla\mathbf{u}_f + \nabla\mathbf{u}_f^T)/2$ is the rate of deformation tensor. The physical parameters involved are the water storage coefficient S , the hydraulic conductivity tensor \mathbb{K} , and the kinematic viscosity of the fluid ν . For simplicity, we assume homogeneous Dirichlet boundary conditions for the hydraulic head ϕ and the free flow velocity \mathbf{u}_f in the conduit except on the interface Γ . On the interface Γ , we impose the continuity of normal velocity (for conservation of mass), the balance of normal component of the normal stress, and the Beavers-Joseph-Saffman-Jones interface boundary conditions (BJSJ) [6, 31, 44]:

$$\begin{cases} \mathbf{u}_f \cdot \mathbf{n}_f = \mathbf{u}_p \cdot \mathbf{n}_f = -(\mathbb{K}\nabla\phi) \cdot \mathbf{n}_f \\ -\boldsymbol{\tau}_j \cdot (\mathbb{T}(\mathbf{u}_f, p_f) \cdot \mathbf{n}_f) = \alpha_{BJSJ}\boldsymbol{\tau}_j \cdot \mathbf{u}_f, \quad j = 1, \dots, d-1 \\ -\mathbf{n}_f \cdot (\mathbb{T}(\mathbf{u}_f, p_f) \cdot \mathbf{n}_f) = g\phi. \end{cases} \quad (2)$$

62 In (2), \mathbf{n}_f denotes the outer normal vector to Ω_f and $\{\boldsymbol{\tau}_j\}$, $j = 1, 2, \dots, d-1$,
63 denotes a set of linearly-independent tangential vectors on the interface Γ .
64 The additional physical parameters are the gravitational constant g and the
65 Beavers-Joseph-Saffman-Jones coefficient $\alpha_{BJSJ} = \frac{\tilde{\alpha}_{BJSJ}\sqrt{d\nu}}{\sqrt{\text{trace}(\mathbb{K})}}$.

Weak formulation of the Stokes-Darcy system. Let $(\cdot, \cdot)_D$ and $\|\cdot\|_D$ denote the standard $L^2(D)$ inner product and norm, respectively, where D can be Ω_p , Ω_f , or Γ . We omit D whenever there is no ambiguity. We define the function spaces

$$\begin{aligned} \mathbf{H}_f &= \left\{ \mathbf{v} \in (H^1(\Omega_f))^d \mid \mathbf{v} = \mathbf{0} \text{ on } \partial\Omega_f \setminus \Gamma \right\}, \\ H_p &= \left\{ \psi \in H^1(\Omega_p) \mid \psi = 0 \text{ on } \partial\Omega_p \setminus \Gamma \right\}, \\ Q &= L^2(\Omega_f), \quad \mathbf{W} = \mathbf{H}_f \times H_p. \end{aligned}$$

66 Let X' denote the dual space of X with respect to the duality induced by
67 the L^2 inner product. The X', X action is denoted by $\langle \cdot, \cdot \rangle_{X', X}$ with the
68 subscript omitted if it is clear from the context.

A weak formulation of the Stokes-Darcy system is then derived by the following procedure. First, we multiply the three equations in (1) by three test functions $\mathbf{v} \in \mathbf{H}_f$, $g\psi \in H_p$, and $q \in Q$, respectively, and integrate the results over each corresponding domain. Then, integration by parts is applied to the terms involving second order derivatives, a process that produces boundary integrals. Finally, we appropriately substitute the BJSJ interface boundary conditions (2) into the boundary integral terms to arrive at the weak formulation

$$\begin{aligned} \langle \langle \underline{\mathbf{u}}_t, \underline{\mathbf{v}} \rangle \rangle + a(\underline{\mathbf{u}}, \underline{\mathbf{v}}) + b(\mathbf{v}, p) + a_\Gamma(\underline{\mathbf{u}}, \underline{\mathbf{v}}) &= \langle \underline{\mathbf{f}}, \underline{\mathbf{v}} \rangle \quad \forall \underline{\mathbf{v}} \in \mathbf{W}, \\ b(\mathbf{u}, q) &= 0 \quad \forall q \in Q, \end{aligned} \quad (3)$$

where $\mathbf{W} = \mathbf{H}_f \times H_p$, $\mathbf{u} = [\mathbf{u}, \phi]^T$, $\mathbf{v} = [\mathbf{v}, \psi]^T$, $\mathbf{f} = [\mathbf{f}, gf]^T$, $(\cdot)_t = \partial(\cdot)/\partial t$,

$$\begin{aligned} \langle \langle \mathbf{u}_t, \mathbf{v} \rangle \rangle &= \langle \mathbf{u}_t, \mathbf{v} \rangle_{\Omega_f} + gS \langle \phi_t, \psi \rangle_{\Omega_p}, & b(\mathbf{v}, q) &= -(q, \nabla \cdot \mathbf{v})_{\Omega_f}, \\ a(\mathbf{u}, \mathbf{v}) &= a_f(\mathbf{u}, \mathbf{v}) + a_p(\phi, \psi) + a_{BJSJ}(\mathbf{u}, \mathbf{v}), \\ a_\Gamma(\mathbf{u}, \mathbf{v}) &= g(\phi, \mathbf{v} \cdot \mathbf{n}_f)_\Gamma - g(\mathbf{u} \cdot \mathbf{n}_f, \psi)_\Gamma, \\ \langle \langle \mathbf{f}, \mathbf{v} \rangle \rangle &= \langle \mathbf{f}, \mathbf{v} \rangle_{\Omega_f} + \langle gf, \psi \rangle_{\Omega_p}, \end{aligned} \quad (4)$$

with

$$\begin{aligned} a_f(\mathbf{u}, \mathbf{v}) &= \nu(\nabla \mathbf{u}, \nabla \mathbf{v})_{\Omega_f}, & a_p(\phi, \psi) &= g(\mathbb{K} \nabla \phi, \nabla \psi)_{\Omega_p} \\ a_{BJSJ}(\mathbf{u}, \mathbf{v}) &= \alpha_{BJSJ}(\mathbf{u} \cdot \boldsymbol{\tau}, \mathbf{v} \cdot \boldsymbol{\tau})_\Gamma. \end{aligned}$$

The bilinear form $a(\cdot, \cdot)$ can be shown to be coercive, i.e.,

$$a(\mathbf{u}, \mathbf{u}) \geq (\nu \|\nabla \mathbf{u}\|^2 + gK_{\min} \|\nabla \phi\|^2 + \alpha_{BJSJ} \|\mathbf{u} \cdot \boldsymbol{\tau}\|_\Gamma^2) \geq C_a \|\nabla \mathbf{u}\|^2, \quad (5)$$

69 where $C_a = \min(\nu, gK_{\min}) > 0$ and K_{\min} denotes the smallest eigenvalue of
70 \mathbb{K} . Details can be found in, e.g., [8, 16].

For the sake of exposition, we introduce the two norms

$$\|\mathbf{u}\|_a = (a(\mathbf{u}, \mathbf{u}))^{\frac{1}{2}}, \quad \|\mathbf{v}\|_S = (\langle \langle \mathbf{v}, \mathbf{v} \rangle \rangle)^{\frac{1}{2}}.$$

It is easy to see that $\|\mathbf{v}\|_S$ is equivalent to the L^2 norm, i.e.,

$$C_s \|\mathbf{v}\|_S \leq \|\mathbf{v}\| \leq C_S \|\mathbf{v}\|_S, \quad (6)$$

71 where $C_s = \min\{1, \sqrt{gS}\}$ and $C_S = \max\{1, \sqrt{gS}\}$.

Third-order Adams-Moulton-Bashforth IMEX method (AMB3). To define our novel third-order scheme that is unconditionally stable and long-time accurate, we first define two Adams-type difference operators. The first is the novel Adams-Moulton difference operator defined on a $2\Delta t$ mesh

$$D_{AM}v^{n+1} = \frac{2}{3}v^{n+1} + \frac{5}{12}v^{n-1} - \frac{1}{12}v^{n-3}, \quad (7)$$

and the other is the Adams-Bashforth difference operator

$$D_{AB}v^{n+1} = \frac{23}{12}v^n - \frac{4}{3}v^{n-1} + \frac{5}{12}v^{n-2}. \quad (8)$$

72 Note that the Adams-Moulton operator (7) is different from the standard one
73 $\frac{5}{12}v^{n+1} + \frac{2}{3}v^n - \frac{1}{12}v^{n-1}$. The novel form of the Adams-Moulton operator that
74 we adopt here is, due to its dissipativity, crucial to the long-time stability.

The third-order Adams-Moulton-Bashforth method is a combination of the third-order explicit Adams-Bashforth treatment for the coupling term and the novel third-order Adams-Moulton method for the remaining terms. Specifically, we have, for any $\mathbf{v} \in \mathbf{W}$ and $q \in Q$,

$$\begin{aligned} \left\langle \left\langle \frac{\mathbf{u}^{n+1} - \mathbf{u}^n}{\Delta t}, \mathbf{v} \right\rangle \right\rangle &+ \tilde{a}(D_{AM}\mathbf{u}^{n+1}, \mathbf{v}) + b(\mathbf{v}, D_{AM}p^{n+1}) \\ &= \langle D_{AM}\mathbf{f}^{n+1}, \mathbf{v} \rangle - \tilde{a}_\Gamma(D_{AB}\mathbf{u}^{n+1}, \mathbf{v}), \\ b(D_{AM}\mathbf{u}^{n+1}, q) &= 0. \end{aligned} \quad (9)$$

Here the bilinear form $\tilde{a}(\underline{\mathbf{u}}, \underline{\mathbf{v}})$ is defined as

$$\tilde{a}(\underline{\mathbf{u}}, \underline{\mathbf{v}}) = a(\underline{\mathbf{u}}, \underline{\mathbf{v}}) + a_{st}(\underline{\mathbf{u}}, \underline{\mathbf{v}}),$$

where the artificial stabilizing term $a_{st}(\cdot, \cdot)$ is defined as

$$a_{st}(\underline{\mathbf{u}}, \underline{\mathbf{v}}) = \gamma_f(\underline{\mathbf{u}} \cdot \mathbf{n}_f, \underline{\mathbf{v}} \cdot \mathbf{n}_f)_\Gamma + \gamma_p(\phi, \psi)_\Gamma \quad (10)$$

with parameters $\gamma_f, \gamma_p \geq 0$. It is obvious that

$$\tilde{a}(\underline{\mathbf{u}}, \underline{\mathbf{u}}) \geq a(\underline{\mathbf{u}}, \underline{\mathbf{u}}) \geq C_a \|\nabla \underline{\mathbf{u}}\|^2, \quad (11)$$

so that we can define the norm

$$\|\underline{\mathbf{u}}\|_a^2 = \tilde{a}(\underline{\mathbf{u}}, \underline{\mathbf{u}}).$$

The interface term $a_\Gamma(\underline{\mathbf{u}}, \underline{\mathbf{v}})$ is modified by $\tilde{a}_\Gamma(\underline{\mathbf{u}}, \underline{\mathbf{v}})$ as

$$\tilde{a}_\Gamma(\underline{\mathbf{u}}, \underline{\mathbf{v}}) = a_\Gamma(\underline{\mathbf{u}}, \underline{\mathbf{v}}) - a_{st}(\underline{\mathbf{u}}, \underline{\mathbf{v}}).$$

75 Notice that the term a_{st} added to $a(u, v)$ is also subtracted from a_Γ , so we are
 76 not adding any artificial terms at the continuous in-time level. This treatment
 77 leads to a Dupont-Douglas type regularization at time-discrete level. Numerical
 78 evidence suggests that this regularization leads to additional stability.

79 *Efficiency of the scheme.* Note that the only term that couples the Stokes
 80 equation in the conduit with the equation in the matrix is the interface term
 81 \tilde{a}_Γ through a_Γ . Because this coupling term is treated explicitly in our scheme
 82 (9), the scheme is of high efficiency because we only need to solve two decoupled
 83 subproblems at each time step, one Stokes and one Darcy:

- 84 1. At time $t = t_{n+1}$, given $\underline{\mathbf{u}}^n, \underline{\mathbf{u}}^{n-1}, \underline{\mathbf{u}}^{n-2}, \underline{\mathbf{u}}^{n-3}$;
- 85 2. Set $\underline{\mathbf{v}} = [\mathbf{v}, 0]$ so that all the terms involving ϕ^{n+1} vanish and thus we only
 86 need apply a fast Stokes solver to determine $\underline{\mathbf{u}}^{n+1}$;
- 87 3. Set $\underline{\mathbf{v}} = [\mathbf{0}, g\psi]$ so that all the terms involving \mathbf{u}^{n+1} vanish and thus we
 88 only need apply a fast Darcy solver for ϕ^{n+1} ;
- 89 4. Set $n = n + 1$ and return to step 1.

90 The computation of step 2 and 3 can be conducted in a parallel fashion and
 91 one can use legacy Stokes and Darcy codes, respectively, for each step, if one
 92 so desires.

93 **3 Unconditional and long-time stability**

94 *Useful inequalities.* We recall a few inequalities to aid readability.

– Trace inequality: if $\underline{\mathbf{v}} \in \mathbf{W}$, then

$$\|\underline{\mathbf{v}}\|_\Gamma \leq C_{tr} \sqrt{\|\underline{\mathbf{v}}\| \|\nabla \underline{\mathbf{v}}\|}, \quad \|\underline{\mathbf{v}}\|_\Gamma \leq C_{tr} \|\nabla \underline{\mathbf{v}}\|, \quad \|\underline{\mathbf{v}}\|_\Gamma \leq C_{tr} \|\underline{\mathbf{v}}\|_a. \quad (12)$$

– Poincaré inequality: if $\underline{\mathbf{v}} \in \mathbf{W}$, then

$$\|\underline{\mathbf{v}}\| \leq C_P \|\nabla \underline{\mathbf{v}}\|. \quad (13)$$

– Young inequality:

$$a^{\frac{1}{2}} b^{\frac{1}{2}} c \leq \frac{a^2}{64\varepsilon^3} + \varepsilon(b^2 + c^2) \quad \forall a, b, c, \varepsilon > 0. \quad (14)$$

95 – Triangle inequality: $\|a + b\|^{\frac{1}{2}} \leq \|a\|^{\frac{1}{2}} + \|b\|^{\frac{1}{2}}$.

96 Other variants of Young's inequality will also be used.

97 *Useful lemmas.* Here we introduce a few useful lemmas that are useful in the
98 analysis of our schemes.

99 The following estimates follow from the basic inequalities.

Lemma 1 Let $a_\gamma(\cdot, \cdot)$ and $a_{st}(\cdot, \cdot)$ be defined as in (4) and (10), respectively. Then, there exists a constant C_{ct} such that

$$|\tilde{a}_\Gamma(\underline{\mathbf{u}}, \underline{\mathbf{v}})| \leq |a_{st}(\underline{\mathbf{u}}, \underline{\mathbf{v}})| + |a_\Gamma(\underline{\mathbf{u}}, \underline{\mathbf{v}})| \leq C_{ct} \|\underline{\mathbf{u}}\|_\Gamma \|\underline{\mathbf{v}}\|_\Gamma \quad \forall \underline{\mathbf{u}}, \underline{\mathbf{v}} \in \mathbf{W}.$$

Lemma 2 For any $\beta_1 > 0$, $\underline{\mathbf{v}}, \underline{\mathbf{w}} \in \mathbf{W}$, we have

$$|\tilde{a}_\Gamma(\underline{\mathbf{v}}, \underline{\mathbf{w}})| \leq \beta_1 (\|\underline{\mathbf{v}}\|_\alpha^2 + \|\underline{\mathbf{w}}\|_\alpha^2) + \beta_2 \|\underline{\mathbf{v}}\|_S^2, \quad (15)$$

100 where $\beta_2 = \frac{1}{64} \beta_1^{-3} C_S^2 C_{ct}^4 C_{tr}^8 C_a^{-1}$.

Proof By Lemma 1, the equivalence between $\|\cdot\|_S$ and $\|\cdot\|$, (6), (11), and the trace theorem, we have, for any $\underline{\mathbf{v}}, \underline{\mathbf{w}} \in \mathbf{W}$,

$$\begin{aligned} \tilde{a}_\Gamma(\underline{\mathbf{v}}, \underline{\mathbf{w}}) &\leq C_{ct} \|\underline{\mathbf{v}}\|_\Gamma \|\underline{\mathbf{w}}\|_\Gamma \leq C_{ct} C_{tr}^2 \|\underline{\mathbf{v}}\|^{\frac{1}{2}} \|\nabla \underline{\mathbf{v}}\|^{\frac{1}{2}} \|\underline{\mathbf{w}}\|_\alpha \\ &\leq C_S^{\frac{1}{2}} C_{ct} C_{tr}^2 C_a^{-\frac{1}{4}} \|\underline{\mathbf{v}}\|_S^{\frac{1}{2}} \|\underline{\mathbf{v}}\|_\alpha^{\frac{1}{2}} \|\underline{\mathbf{w}}\|_\alpha. \end{aligned} \quad (16)$$

101 The inequality (15) is then obtained by setting $\varepsilon = \beta_1 C_S^{-\frac{1}{2}} C_{ct}^{-1} C_{tr}^{-2} C_a^{\frac{1}{4}}$ in the
102 Young's inequality.

Lemma 3 The interface term $\tilde{a}_\Gamma(D_{AB}\underline{\mathbf{u}}, \underline{\mathbf{u}})$ can be bounded by

$$\begin{aligned} &-2\Delta t \tilde{a}_\Gamma \left(\frac{23}{12} \underline{\mathbf{u}}^n - \frac{4}{3} \underline{\mathbf{u}}^{n-1} + \frac{5}{12} \underline{\mathbf{u}}^{n-2}, \underline{\mathbf{u}}^{n+1} \right) \\ &\leq \frac{1}{12} \Delta t \|\underline{\mathbf{u}}^{n+1}\|_\alpha^2 + \frac{23}{528} \Delta t \|\underline{\mathbf{u}}^n\|_\alpha^2 + \frac{16}{528} \Delta t \|\underline{\mathbf{u}}^{n-1}\|_\alpha^2 + \frac{5}{528} \Delta t \|\underline{\mathbf{u}}^{n-2}\|_\alpha^2 \\ &+ \frac{23}{6} \beta_2 \Delta t \|\underline{\mathbf{u}}^n\|_S^2 + \frac{8}{3} \beta_2 \Delta t \|\underline{\mathbf{u}}^{n-1}\|_S^2 + \frac{5}{6} \beta_2 \Delta t \|\underline{\mathbf{u}}^{n-2}\|_S^2. \end{aligned}$$

Proof Set $\beta_1 = \frac{1}{88}$ in Lemma 2. Then $\beta_2 = 10648C_S^2C_{ct}^4C_{tr}^8C_a^{-1}$ and

$$\begin{aligned}
& -2\Delta t \tilde{a}_\Gamma \left(\frac{23}{12} \underline{\mathbf{u}}^n - \frac{4}{3} \underline{\mathbf{u}}^{n-1} + \frac{5}{12} \underline{\mathbf{u}}^{n-2}, \underline{\mathbf{u}}^{n+1} \right) \\
& \leq \frac{23}{6} \Delta t \left(\beta_2 \|\underline{\mathbf{u}}^n\|_S^2 + \frac{1}{88} \|\underline{\mathbf{u}}^n\|_a^2 + \frac{1}{88} \|\nabla \underline{\mathbf{u}}^{n+1}\|_a^2 \right) \\
& \quad + \frac{8}{3} \Delta t \left(\beta_2 \|\underline{\mathbf{u}}^{n-1}\|_S^2 + \frac{1}{88} \|\nabla \underline{\mathbf{u}}^{n-1}\|_a^2 + \frac{1}{88} \|\nabla \underline{\mathbf{u}}^{n+1}\|_a^2 \right) \\
& \quad + \frac{5}{6} \Delta t \left(\beta_2 \|\underline{\mathbf{u}}^{n-2}\|_S^2 + \frac{1}{88} \|\nabla \underline{\mathbf{u}}^{n-2}\|_a^2 + \frac{1}{88} \|\nabla \underline{\mathbf{u}}^{n+1}\|_a^2 \right) \\
& \leq \frac{1}{12} \Delta t \|\underline{\mathbf{u}}^{n+1}\|_a^2 + \frac{23}{528} \Delta t \|\underline{\mathbf{u}}^n\|_a^2 + \frac{16}{528} \Delta t \|\underline{\mathbf{u}}^{n-1}\|_a^2 + \frac{5}{528} \Delta t \|\underline{\mathbf{u}}^{n-2}\|_a^2 \\
& \quad + \frac{23}{6} \beta_2 \Delta t \|\underline{\mathbf{u}}^n\|_S^2 + \frac{8}{3} \beta_2 \Delta t \|\underline{\mathbf{u}}^{n-1}\|_S^2 + \frac{5}{6} \beta_2 \Delta t \|\underline{\mathbf{u}}^{n-2}\|_S^2
\end{aligned} \tag{17}$$

103 so that the lemma is proved.

Lemma 4 *The interface term $-a_\Gamma(D_{AB}\underline{\mathbf{u}}, \underline{\mathbf{u}}) + a_{st}(D_{AB}\underline{\mathbf{u}} - D_{AM}\underline{\mathbf{u}}, \underline{\mathbf{u}})$ can be bounded by*

$$\begin{aligned}
& -2\Delta t a_\Gamma \left(\frac{23}{12} \underline{\mathbf{u}}^n - \frac{4}{3} \underline{\mathbf{u}}^{n-1} + \frac{5}{12} \underline{\mathbf{u}}^{n-2}, \underline{\mathbf{u}}^{n+1} \right) \\
& + 2\Delta t a_{st} \left(-\frac{2}{3} \underline{\mathbf{u}}^{n+1} + \frac{23}{12} \underline{\mathbf{u}}^n - \frac{7}{4} \underline{\mathbf{u}}^{n-1} + \frac{5}{12} \underline{\mathbf{u}}^{n-2} + \frac{1}{12} \underline{\mathbf{u}}^{n-3}, \underline{\mathbf{u}}^{n+1} \right) \\
& \leq \frac{58\Delta t}{360} \|\underline{\mathbf{u}}^{n+1}\|_a^2 + \frac{27\Delta t}{360} \|\underline{\mathbf{u}}^n\|_a^2 + \frac{21\Delta t}{360} \|\underline{\mathbf{u}}^{n-1}\|_a^2 + \frac{7\Delta t}{360} \|\underline{\mathbf{u}}^{n-2}\|_a^2 \\
& \quad + \frac{\Delta t}{360} \|\underline{\mathbf{u}}^{n-3}\|_a^2 + (C_2 + 2C_3) \Delta t \|\underline{\mathbf{u}}^{n+1} - \underline{\mathbf{u}}^n\|_S^2 + 5C_3 \Delta t \|\underline{\mathbf{u}}^n - \underline{\mathbf{u}}^{n-1}\|_S^2 \\
& \quad + 2C_3 \Delta t \|\underline{\mathbf{u}}^{n-1} - \underline{\mathbf{u}}^{n-2}\|_S^2 + \frac{C_3 \Delta t}{3} \|\underline{\mathbf{u}}^{n-2} - \underline{\mathbf{u}}^{n-3}\|_S^2,
\end{aligned} \tag{18}$$

104 where $C_2 = 4920750C_S^2C_{ct}^4C_{tr}^8C_a^{-1}$ and $C_3 = 3375C_S^2C_{ct}^4C_{tr}^8C_a^{-1}$.

Proof Recall $a_\Gamma(\underline{\mathbf{u}}, \underline{\mathbf{u}}) = 0$. Therefore, the interface term can be rewritten as

$$\begin{aligned}
& -2\Delta t a_\Gamma \left(2\underline{\mathbf{u}}^{n+1} + \frac{23}{12} \underline{\mathbf{u}}^n - \frac{4}{3} \underline{\mathbf{u}}^{n-1} + \frac{5}{12} \underline{\mathbf{u}}^{n-2}, \underline{\mathbf{u}}^{n+1} \right) \\
& + 2\Delta t a_{st} \left(-\frac{2}{3} \underline{\mathbf{u}}^{n+1} + \frac{23}{12} \underline{\mathbf{u}}^n - \frac{7}{4} \underline{\mathbf{u}}^{n-1} + \frac{5}{12} \underline{\mathbf{u}}^{n-2} + \frac{1}{12} \underline{\mathbf{u}}^{n-3}, \underline{\mathbf{u}}^{n+1} \right) \\
& = 2\Delta t a_\Gamma (\underline{\mathbf{u}}^{n+1} - \underline{\mathbf{u}}^n, \underline{\mathbf{u}}^{n+1}) - \frac{11}{6} \Delta t a_\Gamma (\underline{\mathbf{u}}^n - \underline{\mathbf{u}}^{n-1}, \underline{\mathbf{u}}^{n+1}) \\
& \quad + \frac{5}{6} \Delta t a_\Gamma (\underline{\mathbf{u}}^{n-1} - \underline{\mathbf{u}}^{n-2}, \underline{\mathbf{u}}^{n+1}) - \frac{4}{3} \Delta t a_{st} (\underline{\mathbf{u}}^{n+1} - \underline{\mathbf{u}}^n, \underline{\mathbf{u}}^{n+1}) \\
& \quad + \frac{5}{2} \Delta t a_{st} (\underline{\mathbf{u}}^n - \underline{\mathbf{u}}^{n-1}, \underline{\mathbf{u}}^{n+1}) - \Delta t a_{st} (\underline{\mathbf{u}}^{n-1} - \underline{\mathbf{u}}^{n-2}, \underline{\mathbf{u}}^{n+1}) \\
& \quad - \frac{1}{6} \Delta t a_{st} (\underline{\mathbf{u}}^{n-2} - \underline{\mathbf{u}}^{n-3}, \underline{\mathbf{u}}^{n+1}).
\end{aligned} \tag{19}$$

Similar as in the proof of Lemma 2, the first term on the right-hand side can be estimated by

$$2\Delta t a_T (\mathbf{u}^{n+1} - \mathbf{u}^n, \mathbf{u}^{n+1}) \leq \frac{\Delta t}{180} \|\mathbf{u}^{n+1}\|_a^2 + C_2 \Delta t \|\mathbf{u}^{n+1} - \mathbf{u}^n\|_S^2 \quad (20)$$

105 and the other terms can be directly estimated by Lemma 2 with $\beta_1 = \frac{1}{60}$. The
106 desired result (18) then follows easily.

107 The following variants of the Grownwall-Bellman inequality will simplify
108 the analysis. They are particularly useful for the stability analysis of multi-step
109 methods.

Lemma 5 *Assume that $\{z_n\}$ and $\{y_n\}$ are two non-negative sequences that satisfy*

$$z_{n+1} + \xi_{-1} y_{n+1} \leq z_n + \Delta t \sum_{i=0}^k \zeta_i z_{n-i} + \sum_{i=0}^k \xi_i y_{n-i} + \Delta t \bar{z}, \quad (21)$$

where \bar{z} , ξ_i , and ζ_i are nonnegative constants and

$$\xi_{-1} \geq \sum_{i=0}^k \xi_i. \quad (22)$$

Let

$$E_n = z_n + \frac{\Delta t}{1 + \Delta t \sum_{i=0}^k \zeta_i} \sum_{i=1}^k \sum_{j=i}^k \zeta_j z_{n-i} + \frac{1}{1 + \Delta t \sum_{i=0}^k \zeta_i} \sum_{i=0}^k \sum_{j=i}^k \xi_j y_{n-i}. \quad (23)$$

Then

$$E_n \leq e^{\sum_{i=0}^k \zeta_i t} \left(E_k + \frac{\bar{z}}{\sum_{i=0}^k \zeta_i} \right) \quad (24)$$

110 for any $n\Delta t \leq t$.

Proof From the definition of E_n and the constraint (22), we have

$$E_{n+1} \leq (1 + \Delta t \sum_{i=0}^k \zeta_i) E_n + \Delta t \bar{z} \quad (25)$$

111 so that the bound (24) is easily derived via recursion.

112 Another variant of Grownwall-Bellman inequality will be useful in the long
113 time stability analysis.

Lemma 6 Assume that $\{z_n\}$ and $\{y_n\}$ are two nonnegative sequences that satisfy

$$z_{n+1} + \zeta_{-1}\Delta t y_{n+1} \leq z_n + \Delta t \sum_{i=0}^k \zeta_i y_{n-i} + \Delta t \bar{z}, \quad (26)$$

where ζ_i , $i = -1, \dots, k$, are nonnegative constants and

$$\bar{\zeta} = \frac{1}{k+1} \left(\zeta_{-1} - \sum_{i=0}^k \zeta_i \right) > 0. \quad (27)$$

Let

$$E_n = z_n + \Delta t \sum_{i=0}^k \left((k-i)\bar{\zeta} + \sum_{j=i}^k \zeta_j \right) y_{n-i}. \quad (28)$$

Then

$$E_{n+1} + \bar{\zeta}\Delta t \sum_{i=0}^k y_{n+1-i} \leq E_n + \Delta t \bar{z}. \quad (29)$$

Moreover, if $z_{n+1} \leq C_\zeta y_{n+1}$, then

$$E_n \leq (1 + \bar{C}\Delta t)^{-(n-k)} E_k + \frac{\bar{z}}{\bar{C}}, \quad (30)$$

where

$$\bar{C} = \min \left\{ \frac{\bar{\zeta}}{2C_\zeta}, \frac{\bar{\zeta}}{2(\zeta_{-1} - \bar{\zeta})\Delta t} \right\}. \quad (31)$$

114 *Proof* Let $d_i = (k-i)\bar{\zeta} + \sum_{j=i}^k \zeta_j$. Then $E_n = z_n + \Delta t \sum_{i=0}^k d_i y_{n-i}$. It is easily
115 verified that

$$d_0 + \bar{\zeta} = \zeta_{-1}, \quad (32)$$

$$d_i - d_{i+1} - \bar{\zeta} = \zeta_i, \quad \text{for } i = 1, \dots, k-1, \quad (33)$$

$$d_k = \zeta_k, \quad (34)$$

so the inequality (26) can be recast as

$$z_{n+1} + \Delta t (d_0 + \bar{\zeta}) y_{n+1} \leq z_n + \Delta t \sum_{i=0}^{k-1} (d_i - d_{i+1} - \bar{\zeta}) y_{n-i} + \Delta t d_k y_{n-k} + \Delta t \bar{z} \quad (35)$$

or

$$z_{n+1} + \Delta t \sum_{i=0}^k d_i y_{n+1-i} + \bar{\zeta}\Delta t \sum_{i=0}^k y_{n+1-i} \leq z_n + \Delta t \sum_{i=0}^k d_i y_{n-i} + \Delta t \bar{z}, \quad (36)$$

116 which is exactly the inequality (29). Now, if $z_{n+1} \leq C_\zeta y_{n+1}$, then

$$\begin{aligned} \sum_{i=0}^k y_{n+1-i} &\geq \frac{1}{2C_\zeta} z_{n+1} + \frac{y_{n+1}}{2} + \sum_{i=1}^k y_{n+1-i} \\ &\geq \frac{1}{2C_\zeta} z_{n+1} + \Delta t \tilde{C} \sum_{i=0}^k d_i y_{n+1-i}, \end{aligned} \quad (37)$$

where $\tilde{C} = \frac{1}{\Delta t} \min\{\frac{1}{2d_0}, \min\{d_i^{-1}\}_{i=1}^k\} = \frac{1}{2d_0 \Delta t}$. Note that $d_0 = k\bar{\zeta} + \sum_{j=0}^k \zeta_j = \zeta_{-1} - \bar{\zeta}$ so that

$$\bar{\zeta} \sum_{i=0}^k y_{n+1-i} \geq \bar{C} (z_{n+1} + \Delta t \sum_{i=0}^k d_i y_{n+1-i}) = \bar{C} E_{n+1}, \quad (38)$$

where \bar{C} is defined in (31). Then, from (29), we have

$$(1 + \bar{C} \Delta t) E_{n+1} \leq E_n + \Delta t \bar{z}. \quad (39)$$

117 Now by recursion, we have

$$\begin{aligned} E_n &\leq (1 + \bar{C} \Delta t)^{-(n-k)} E_k + \Delta t \bar{z} \sum_{i=1}^{n-k} (1 + \bar{C} \Delta t)^{-i} \\ &\leq (1 + \bar{C} \Delta t)^{-(n-k)} E_k + \frac{\bar{z}}{\bar{C}} \end{aligned} \quad (40)$$

118 so that the lemma is proved.

119 Additional sequences are considered in the following lemma.

Lemma 7 Assume that $\{z_n\}$ and $\{y_n^\ell\}$, $\ell = 1, \dots, L$, are nonnegative sequences that satisfy

$$z_{n+1} + \Delta t \sum_{\ell=1}^L \zeta_{-1}^\ell y_{n+1}^\ell \leq z_n + \Delta t \sum_{\ell=1}^L \sum_{i=0}^{k_\ell} \zeta_i^\ell y_{n-i}^\ell + \Delta t \bar{z}, \quad (41)$$

where ζ_i^ℓ , $\ell = 1, \dots, L$ and $i = -1, \dots, k_\ell$, are nonnegative constants with $1 \leq k_\ell \leq k$, and

$$\bar{\zeta}^\ell = \frac{1}{k_\ell + 1} \left(\zeta_{-1}^\ell - \sum_{i=0}^{k_\ell} \zeta_i^\ell \right) > 0. \quad (42)$$

Define

$$E_n = z_n + \Delta t \sum_{\ell=1}^L \sum_{i=0}^{k_\ell} \left((k_\ell - i) \bar{\zeta}^\ell + \sum_{j=i}^{k_\ell} \zeta_j^\ell \right) y_{n-i}^\ell. \quad (43)$$

Then

$$E_{n+1} + \Delta t \sum_{\ell=1}^L \bar{\zeta}^\ell \sum_{i=0}^{k_\ell} y_{n+1-i}^\ell \leq E_n + \Delta t \bar{z}. \quad (44)$$

In addition, assume that $z_{n+1} \leq C_\zeta y_{n+1}^{\ell_0}$ for some ℓ_0 . Then

$$E_n \leq (1 + \bar{C}\Delta t)^{-(n-k)} E_k + \frac{\bar{z}}{\bar{C}}, \quad (45)$$

where

$$\bar{C} = \min \left\{ \frac{\bar{\zeta}^{\ell_0}}{2C_\zeta}, \min_\ell \frac{\bar{\zeta}^\ell}{2(\bar{\zeta}^{\ell-1} - \bar{\zeta}^\ell)\Delta t} \right\}. \quad (46)$$

120 The proof is very much the same as that for Lemma 6 and thus is omitted
121 here.

122 *Unconditional stability.* Now we can prove that our novel AMB3 scheme is
123 unconditionally stable over any finite time.

124 **Theorem 1** *Let $T > 0$ be any fixed time. Then, the AMB3 scheme (9) is*
125 *unconditionally stable in $(0, T]$.*

Proof Set $\underline{\mathbf{v}} = 2\Delta t \underline{\mathbf{u}}^{n+1}$ in (9). Using of $\langle 2a, a - b \rangle = |a|^2 + |a - b|^2 - |b|^2$, we obtain

$$\begin{aligned} & \|\underline{\mathbf{u}}^{n+1}\|_S^2 - \|\underline{\mathbf{u}}^n\|_S^2 + \|\underline{\mathbf{u}}^{n+1} - \underline{\mathbf{u}}^n\|_S^2 + 2\Delta t \tilde{a} (D_{AM} \underline{\mathbf{u}}^{n+1}, \underline{\mathbf{u}}^{n+1}) \\ &= 2\Delta t \langle D_{AM} \underline{\mathbf{f}}^{n+1}, \underline{\mathbf{u}}^{n+1} \rangle - 2\Delta t \tilde{a}_\Gamma (D_{AB} \underline{\mathbf{u}}^{n+1}, \underline{\mathbf{u}}^{n+1}), \end{aligned} \quad (47)$$

where the pressure term $b(\underline{\mathbf{u}}^{n+1}, \frac{2}{3}p^{n+1} + \frac{5}{12}p^{n-1} - \frac{1}{12}p^{n-3}) = 0$ because $\underline{\mathbf{u}}^{n+1} \in \mathbf{H}_f$ and $p^{n+1}, p^{n-1}, p^{n-3} \in \mathbf{Q}$. A crucial observation is that the last term on the left-hand-side can be bounded below, i.e., according to Young's inequality, we have

$$\begin{aligned} & 2\tilde{a} \left(\frac{2}{3} \underline{\mathbf{u}}^{n+1} + \frac{5}{12} \underline{\mathbf{u}}^{n-1} - \frac{1}{12} \underline{\mathbf{u}}^{n-3}, \underline{\mathbf{u}}^{n+1} \right) \\ & \geq 2 \left(\frac{2}{3} \|\underline{\mathbf{u}}^{n+1}\|_{\tilde{a}}^2 - \frac{5}{24} (\|\underline{\mathbf{u}}^{n-1}\|_{\tilde{a}}^2 + \|\underline{\mathbf{u}}^{n+1}\|_{\tilde{a}}^2) - \frac{1}{24} (\|\underline{\mathbf{u}}^{n-3}\|_{\tilde{a}}^2 + \|\underline{\mathbf{u}}^{n+1}\|_{\tilde{a}}^2) \right) \\ & \geq \frac{5}{6} \|\underline{\mathbf{u}}^{n+1}\|_{\tilde{a}}^2 - \frac{5}{12} t \|\underline{\mathbf{u}}^{n-1}\|_{\tilde{a}}^2 - \frac{1}{12} t \|\underline{\mathbf{u}}^{n-3}\|_{\tilde{a}}^2. \end{aligned} \quad (48)$$

126 This implies that the special Adams-Moulton operator that we developed is
127 dissipative because the coefficient of the positive term is larger than the sum
128 of the coefficients of the negative terms. This fact will be exploited heavily
129 below to prove the unconditional stability as well as the long-time stability of
130 the scheme.

We also notice that the forcing term on the right-hand-side can be bounded above according to Young's inequality:

$$\begin{aligned} 2 \langle D_{AM} \underline{\mathbf{f}}^{n+1}, \underline{\mathbf{u}}^{n+1} \rangle & \leq \frac{1}{6C_P^2} C_a \|\underline{\mathbf{u}}^{n+1}\|^2 + 6C_P^2 C_a^{-1} \|D_{AM} \underline{\mathbf{f}}^{n+1}\|^2 \\ & \leq \frac{1}{6} \|\underline{\mathbf{u}}^{n+1}\|_{\tilde{a}}^2 + \beta_3 \max_i \|\underline{\mathbf{f}}^i\|^2, \end{aligned} \quad (49)$$

where $\beta_3 = 10C_P^2 C_a^{-1}$. Combining the above estimates with Lemma 3 and discarding the term $\|\underline{\mathbf{u}}^{n+1} - \underline{\mathbf{u}}^n\|_S^2$, we have

$$\begin{aligned} & \|\underline{\mathbf{u}}^{n+1}\|_S^2 + \frac{308}{528}\Delta t \|\underline{\mathbf{u}}^{n+1}\|_a^2 \\ & \leq (1 + \frac{23}{6}\beta_2\Delta t)\|\underline{\mathbf{u}}^n\|_S^2 + \frac{8}{3}\beta_2\Delta t\|\underline{\mathbf{u}}^{n-1}\|_S^2 + \frac{5}{6}\beta_2\Delta t\|\underline{\mathbf{u}}^{n-2}\|_S^2 + \frac{23}{528}\Delta t\|\underline{\mathbf{u}}^n\|_a^2 \\ & \quad + \frac{236}{528}\Delta t\|\underline{\mathbf{u}}^{n-1}\|_a^2 + \frac{5}{528}\Delta t\|\underline{\mathbf{u}}^{n-2}\|_a^2 + \frac{44}{528}\Delta t\|\underline{\mathbf{u}}^{n-3}\|_a^2 + \beta_3\Delta t \max_i \|\underline{\mathbf{f}}^i\|^2. \end{aligned}$$

Now, define

$$\begin{aligned} E_n &= \|\underline{\mathbf{u}}^n\|_S^2 + \frac{7\beta_2\Delta t}{2(1 + \frac{22}{3}\beta_2\Delta t)}\|\underline{\mathbf{u}}^{n-1}\|_S^2 + \frac{5\beta_2\Delta t}{6(1 + \frac{22}{3}\beta_2\Delta t)}\|\underline{\mathbf{u}}^{n-2}\|_S^2 \\ & \quad + \frac{308\Delta t}{528(1 + \frac{22}{3}\beta_2\Delta t)}\|\underline{\mathbf{u}}^n\|_a^2 + \frac{285\Delta t}{528(1 + \frac{22}{3}\beta_2\Delta t)}\|\underline{\mathbf{u}}^{n-1}\|_a^2 \\ & \quad + \frac{49\Delta t}{528(1 + \frac{22}{3}\beta_2\Delta t)}\|\underline{\mathbf{u}}^{n-2}\|_a^2 + \frac{44\Delta t}{528(1 + \frac{22}{3}\beta_2\Delta t)}\|\underline{\mathbf{u}}^{n-3}\|_a^2. \end{aligned} \quad (50)$$

We then have, by Lemma 5

$$\|\underline{\mathbf{u}}^{n+1}\|_S^2 \leq E_n \leq e^{\frac{22}{3}\beta_2 T} \left(E_3 + \frac{3\beta_3}{22\beta_2} \max_i \|\underline{\mathbf{f}}^i\|^2 \right), \quad (51)$$

131 on any finite time interval $[0, T]$.

132 *Long-time stability.* We next show that our scheme is long-time stable in the
133 sense that the solutions will remain bounded uniformly in time as long as
134 a time-step restriction is satisfied. As a direct consequence of this long-time
135 stability, we are able to show that we are able to derive uniform in time bounds
136 on the error.

Theorem 2 *Assume that $\mathbf{f} \in L^\infty(L^2(\Omega))$. For the AMB3 scheme, there exists $\Delta t_0 > 0$ such that the solution is uniformly bounded in time if $\Delta t \leq \Delta t_0$. In particular, there exist $0 < \lambda_1 < 1, 0 < \lambda_2 < \infty$, and $E_3 \geq 0$ such that*

$$\|\underline{\mathbf{u}}^{n+1}\|^2 \leq \lambda_1^{n-2} E_3 + \lambda_2.$$

Proof After rearranging (47) in a slightly different way, we have

$$\begin{aligned} & \|\underline{\mathbf{u}}^{n+1}\|_S^2 - \|\underline{\mathbf{u}}^n\|_S^2 + \|\underline{\mathbf{u}}^{n+1} - \underline{\mathbf{u}}^n\|_S^2 + 2\Delta t a (D_{AM}\underline{\mathbf{u}}^{n+1}, \underline{\mathbf{u}}^{n+1}) \\ & = 2\Delta t \langle D_{AM}\underline{\mathbf{f}}^{n+1}, \underline{\mathbf{u}}^{n+1} \rangle - 2\Delta t a_\Gamma (D_{AB}\underline{\mathbf{u}}^{n+1}, \underline{\mathbf{u}}^{n+1}) \\ & \quad + 2\Delta t a_{st} (D_{AB}\underline{\mathbf{u}}^{n+1} - D_{AM}\underline{\mathbf{u}}^{n+1}, \underline{\mathbf{u}}^{n+1}). \end{aligned} \quad (52)$$

Similar to the proof of the previous theorem, the bilinear term on the left-hand-side can be bounded from below by

$$2a (D_{AM}\underline{\mathbf{u}}^{n+1}, \underline{\mathbf{u}}^{n+1}) \geq \frac{5}{6}\|\underline{\mathbf{u}}^{n+1}\|_a^2 - \frac{5}{12}\|\underline{\mathbf{u}}^{n-1}\|_a^2 - \frac{1}{12}\|\underline{\mathbf{u}}^{n-3}\|_a^2 \quad (53)$$

and the forcing term can be bounded from above by

$$2 \langle D_{AM} \mathbf{f}^{n+1}, \mathbf{u}^{n+1} \rangle \leq \frac{1}{180} \|\mathbf{u}^{n+1}\|_a^2 + \beta_4 \max_i \|\mathbf{f}^i\|^2, \quad (54)$$

where $\beta_4 = 300C_P^2C_a^{-1}$. The interface term has been estimated in Lemma 4. Combine the above inequalities with Lemma 4, we have

$$\begin{aligned} & \|\mathbf{u}^{n+1}\|_S^2 + \frac{240}{360} \Delta t \|\mathbf{u}^{n+1}\|_a^2 + [1 - (C_2 + 2C_3)\Delta t] \|\mathbf{u}^{n+1} - \mathbf{u}^n\|_S^2 \\ & \leq \|\mathbf{u}^n\|_S^2 + \frac{27}{360} \Delta t \|\mathbf{u}^n\|_a^2 + \frac{171}{360} \Delta t \|\mathbf{u}^{n-1}\|_a^2 + \frac{7}{360} \Delta t \|\mathbf{u}^{n-2}\|_a^2 \\ & + \frac{31}{360} \Delta t \|\mathbf{u}^{n-3}\|_a^2 + 5C_3 \Delta t \|\mathbf{u}^n - \mathbf{u}^{n-1}\|_S^2 + 2C_3 \Delta t \|\mathbf{u}^{n-1} - \mathbf{u}^{n-2}\|_S^2 \\ & + \frac{C_3 \Delta t}{3} \|\mathbf{u}^{n-2} - \mathbf{u}^{n-3}\|_S^2 + \beta_4 \Delta t \max_i \|\mathbf{f}^i\|^2. \end{aligned} \quad (55)$$

We require that

$$1 - (C_2 + 2C_3)\Delta t > \frac{25C_3}{3} \Delta t. \quad (56)$$

A convenient choice is

$$\Delta t_0 \leq \frac{1}{C_2 + \frac{31}{3}C_3} \quad (57)$$

such that $1 - (C_2 + 2C_3)\Delta t \geq \frac{25C_3}{3} \Delta t$ if $\Delta t \leq \Delta t_0$. Let

$$\begin{aligned} E_n &= \|\mathbf{u}^n\|_S^2 + \frac{239}{360} \Delta t \|\mathbf{u}^n\|_a^2 + \frac{211}{360} \Delta t \|\mathbf{u}^{n-1}\|_a^2 + \frac{39}{360} \Delta t \|\mathbf{u}^{n-2}\|_a^2 \\ & + \frac{31}{360} \Delta t \|\mathbf{u}^{n-3}\|_a^2 + \frac{24C_3 \Delta t}{3} \|\mathbf{u}^n - \mathbf{u}^{n-1}\|_S^2 \\ & + \frac{8C_3 \Delta t}{3} \|\mathbf{u}^{n-1} - \mathbf{u}^{n-2}\|_S^2 + \frac{C_3 \Delta t}{3} \|\mathbf{u}^{n-2} - \mathbf{u}^{n-3}\|_S^2. \end{aligned} \quad (58)$$

Note that $\|\mathbf{u}^{n+1}\|_S^2 \leq C_\zeta \|\mathbf{u}^{n+1}\|_a^2$, where $C_\zeta = C_P^2 C_a^{-2} C_s^{-2}$. By Lemma 7, we arrive at the conclusion

$$\|\mathbf{u}^{n+1}\|_S^2 \leq E_{n+1} \leq (1 + \bar{C}\Delta t)^{n-2} E_3 + \bar{C}^{-1} \beta_4 \max_i \|\mathbf{f}^i\|^2, \quad (59)$$

137 where $\bar{C} = \min\{\frac{1}{720C_\zeta}, \frac{1}{478}\}$. The theorem is proven if we set $\lambda_1 = (1 + \bar{C}\Delta t)^{-1}$
138 and $\lambda_2 = \bar{C}^{-1} \beta_4 \max_i \|\mathbf{f}^i\|^2$.

139 An immediate consequence of the previous theorem is the following uniform
140 in time error bound. This is a highly desirable property because the retention
141 and release of contaminants in karst aquifers usually occur over very long time
142 scales.

Theorem 3 *Suppose that the solutions $\underline{\mathbf{u}}$ and p are smooth and bounded uniformly in time. Let $\underline{\mathbf{e}}^n := \underline{\mathbf{u}}(n\Delta t) - \underline{\mathbf{u}}^n$ denote the error. Then, provided that the time-step restriction as in the previous theorem is satisfied, we have the estimates*

$$\|\underline{\mathbf{e}}^{n+1}\|^2 \leq (1 + \bar{C}\Delta t)^{-n+2}\epsilon_3^2 + C_4(\Delta t)^6,$$

where \bar{C} and C_4 are appropriate positive constants, and

$$\begin{aligned} \epsilon_3^2 &= \|\underline{\mathbf{e}}^3\|_S^2 + \frac{239}{360}\Delta t\|\underline{\mathbf{e}}^3\|_a^2 + \frac{211}{360}\Delta t\|\underline{\mathbf{e}}^2\|_a^2 + \frac{39}{360}\Delta t\|\underline{\mathbf{e}}^1\|_a^2 \\ &+ \frac{24C_3\Delta t}{3}\|\underline{\mathbf{e}}^3 - \underline{\mathbf{e}}^2\|_S^2 + \frac{8C_3\Delta t}{3}\|\underline{\mathbf{e}}^2 - \underline{\mathbf{e}}^1\|_S^2 + \frac{C_3\Delta t}{3}\|\underline{\mathbf{e}}^1\|_S^2. \end{aligned}$$

Proof Because $\underline{\mathbf{u}}, p$ are smooth and bounded, and since the scheme 9 is third-order in time, we have that the solution satisfies the scheme in the form of

$$\begin{aligned} &\left\langle \left\langle \frac{\underline{\mathbf{u}}((n+1)\Delta t) - \underline{\mathbf{u}}(n\Delta t)}{\Delta t}, \underline{\mathbf{v}} \right\rangle \right\rangle + \tilde{a}(D_{\text{AM}}\underline{\mathbf{u}}((n+1)\Delta t), \underline{\mathbf{v}}) \\ &+ b(\underline{\mathbf{v}}, D_{\text{AMP}}((n+1)\Delta t)) = \langle D_{\text{AM}}\underline{\mathbf{f}}^{n+1}, \underline{\mathbf{v}} \rangle - \tilde{a}_\Gamma(D_{\text{AB}}\underline{\mathbf{u}}((n+1)\Delta t), \underline{\mathbf{v}}) \\ &+ (R^{n+1}, \underline{\mathbf{v}}), \\ &b(D_{\text{AM}}\underline{\mathbf{u}}((n+1)\Delta t), q) = 0, \end{aligned}$$

where the remainder term R^n is uniformly bounded by

$$\|R^n\| \leq C(\Delta t)^3 \quad \forall n = 1, 2, \dots$$

This implies that the error $\underline{\mathbf{e}}^n$ satisfies

$$\begin{aligned} &\left\langle \left\langle \frac{\underline{\mathbf{e}}^{n+1} - \underline{\mathbf{e}}^n}{\Delta t}, \underline{\mathbf{v}} \right\rangle \right\rangle + \tilde{a}(D_{\text{AM}}\underline{\mathbf{e}}^{n+1}, \underline{\mathbf{v}}) + b(\underline{\mathbf{v}}, D_{\text{AM}}e_p^{n+1}) \\ &= -\tilde{a}_\Gamma(D_{\text{AB}}\underline{\mathbf{e}}^{n+1}, \underline{\mathbf{v}}) + (R^{n+1}, \underline{\mathbf{v}}), \\ &b(D_{\text{AM}}\underline{\mathbf{e}}^{n+1}, q) = 0, \end{aligned}$$

143 where $e_p^n = p(n\Delta t) - p^n$. Repeating the same argument as in the previous
144 theorem leads to the desired estimate. Therefore, we have a third-order uniform
145 in time error bound provided that the time-step restriction is satisfied and that
146 the scheme is initiated properly so that ϵ_3 is of third-order. This ends the proof
147 of uniform in time third-order error bound.

148 **Remark 4** *If a conforming finite element is used, the scheme is still long-*
149 *time stable under the constraint $\Delta t \leq \Delta t_0$ where Δt_0 is independent of the*
150 *finite element mesh size h . Moreover, based on the stability analysis, we can*
151 *prove that the AMB3 scheme is third-order temporal accurate. Following the*
152 *analysis in [16], if the Taylor-Hood (P2-P1) finite element pair is used for the*
153 *discretization of the Stokes system and continuous piecewise quadratic (P2)*
154 *finite elements are used for discretization of the Darcy system, the error of the*
155 *fully discretized scheme will be $\|\underline{\mathbf{u}}^n(t) - \underline{\mathbf{u}}_h^n\| = O(\Delta t^3 + h^3)$, which is illustrated*
156 *by the numerical results in next section.*

157 4 Numerical results

158 We report here on the results of several numerical experiments. The numerical
159 results illustrate the third-order accuracy, unconditional stability, and the long-
160 time stability and uniform in time error bounds.

Suppose that the error behaves like $O(h^{\theta_1} + \Delta t^{\theta_2})$. Then, if we set $\Delta t = h^\theta$, the rate of convergence would be of the order of $r_{h,\theta} = \min(\theta_1, \theta\theta_2)$ with respect to h . The rate of convergence can be numerically estimated by calculating

$$r_{h,\theta} \approx \log_2 \frac{\|u_{2h,\theta} - u_{exact}\|_{l^2}}{\|u_{h,\theta} - u_{exact}\|_{l^2}}. \quad (60)$$

161 Here, we use the discrete l^2 norm of nodal values to measure errors.

162 We set $\Omega_f = (0, 1) \times (1, 2)$, $\Omega_p = (0, 1) \times (0, 1)$, and the interface $\Gamma = (0, 1) \times$
163 $\{1\}$ which separates Ω_f and Ω_p . Uniform triangular meshes are created by first
164 dividing the rectangular domains Ω_p and Ω_f into identical small squares and
165 then dividing each square into two triangles. With respect to such grids, the
166 Taylor-Hood (P2-P1) finite element pair is used to discretize the Stokes system
167 so that the conduit fluid velocity \mathbf{u}_h is approximated by continuous piecewise
168 quadratic functions and the conduit pressure p is approximated by continuous
169 piecewise linear functions. Continuous piecewise quadratic functions are used
170 to approximate the hydraulic head ϕ_h .

171 4.1 Convergence rates

We choose the manufactured solution of the Stokes-Darcy system (1) given by

$$\begin{aligned} \mathbf{u}_f(\mathbf{x}, t) &= \left(-\frac{1}{\pi} e^y \sin \pi x \cos 2\pi t, (e^y - e) \cos \pi x \cos 2\pi t \right), \\ p_f(\mathbf{x}, t) &= 2e^y \cos \pi x \cos 2\pi t, \\ \phi(\mathbf{x}, t) &= (e^y - ey) \cos \pi x \cos 2\pi t. \end{aligned}$$

172 The right-hand side data in the partial differential equations, initial conditions,
173 and boundary conditions are then chosen correspondingly. Here, we set $\Delta t = h$,
174 $\mathbb{K} = \mathbb{I}$, $\nu = g = S = \gamma_f = \gamma_p = 1$, $T = 1$, and $\alpha_{BJSJ} = 1$.

175 Table 1 shows that the numerical convergence rate is approximately third
176 order for ϕ and \mathbf{u} , and of a bit over second order for p . This is all consistent with
177 the third-order temporal scheme and the Taylor-Hood (P2-P1) finite element
178 pair for the Stokes equations and the the P2 element for the Darcy equation.

h	e_ϕ	e_u	e_p
1/16	1.40e-3	6.49e-4	1.35e-2
1/32	2.05e-4	9.44e-5	1.97e-3
1/64	2.70e-5	1.24e-5	3.36e-4
1/128	3.45e-6	1.58e-6	6.55e-5
1/256	4.36e-7	1.99e-7	1.41e-5
1/512	5.45e-8	2.49e-8	3.26e-6
$r_{terminal}$	3.00	3.00	2.11

Table 1 Relative error and order of accuracy with respect to the spatial grid size h for Example 4.1 at $t = 1$ and with $\Delta t = h$ and $r_{terminal} = r_{1/512,1}$ defined by (60).

179 4.2 Long-time error

To illustrate the long-time behavior of our schemes, we use the following manufactured solution that is a slight modification of one used in [9]:

$$\begin{aligned} \mathbf{u}_f(\mathbf{x}, t) &= \left([x^2 y^2 + e^{-y}], [-\frac{2}{3} x y^3 + [2 - \pi \sin(\pi x)]] \right) [2 + \cos(2\pi t)] \\ p_f(\mathbf{x}, t) &= -[2 - \pi \sin(\pi x)] \cos(2\pi y) [2 + \cos(2\pi t)] \\ \phi(\mathbf{x}, t) &= [2 - \pi \sin(\pi x)] [-y + \cos(\pi(1 - y))] [2 + \cos(2\pi t)]. \end{aligned}$$

180 The right-hand side data in the partial differential equations, initial conditions,
181 and boundary conditions are then chosen correspondingly. Here, we set $\mathbb{K} = \mathbb{I}$,
182 $\nu = g = S = 1$, $T = 1$, and $\alpha_{BJSJ} = 1$. In this long time numerical experiment,
183 we set the terminal time $T = 100$ and $h = 1/64$. Figure 2 displays the relative
184 error as a function of t for two different values of Δt . We see that the long-time
185 error remains bounded, and indeed, seems to not grow.

186 4.3 Long-time stability analysis

We use the same domain and the same initial conditions as in the Section 4.2, i.e., we have

$$\begin{aligned} \mathbf{u}_f(\mathbf{x}, 0) &= \left(-\frac{1}{\pi} e^y \sin \pi x, (e^y - e) \cos \pi x \right), \\ p_f(\mathbf{x}, 0) &= 2e^y \cos \pi x, \\ \phi(\mathbf{x}, 0) &= (e^y - ey) \cos \pi x, \end{aligned}$$

187 but now the forcing terms are set to zero and homogeneous Dirichlet boundary
188 conditions are imposed on the hydraulic head ϕ and conduit flow velocity
189 \mathbf{u} . To study the long-time stability of the scheme, we define the functionals
190 $E_\phi = \|\phi\|_{l^2}^2$, $E_u = \|\mathbf{u}\|_{l^2}^2$, and $E_p = \|p\|_{l^2}^2$. The final time is set to $T = 100$.

191 For Figure 3, we set $h = 1/128$, $\Delta t = 1/10$, $\mathbb{K} = \mathbb{I}$, $\nu = g = S = 1$, and
192 $\gamma_f = \gamma_p = 0$. The energy does decay as time evolves, which suggests that the
193 long-time stability time-step size constraint in the analysis is satisfied with the
194 above choices for the parameters.

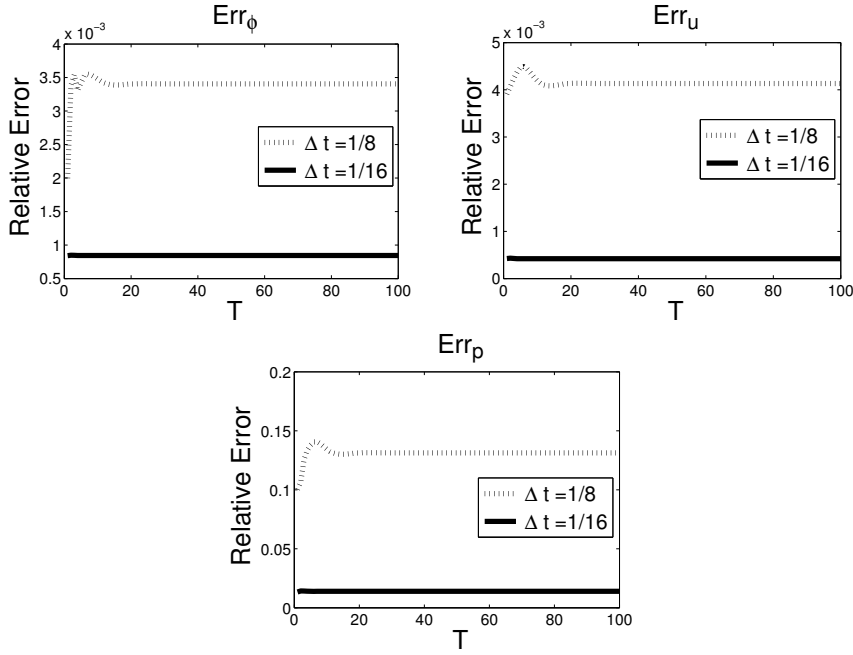


Fig. 2 Relative error for the hydraulic head in the matrix ϕ (top-left), conduit velocity \mathbf{u} (top-right), and conduit pressure p (bottom) for $0 \leq t \leq 100$ for $h = 1/64$.

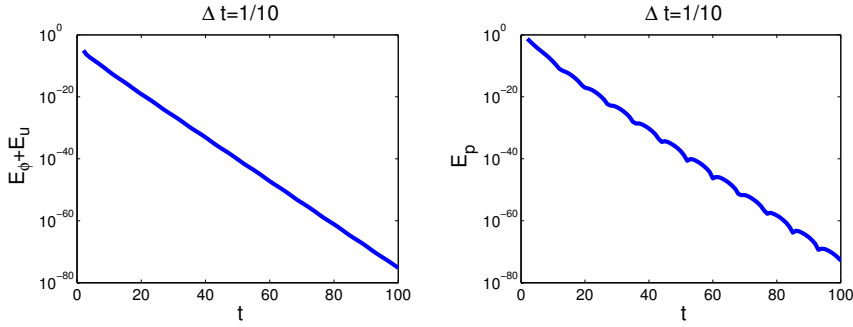


Fig. 3 Long-time behavior of the functionals $E_\phi + E_{\mathbf{u}}$ (left) and E_p (right) for $\nu = 1$ and $\mathbb{K} = \mathbb{I}$.

195 For Figure 4, we set $h = 1/128$, $\mathbb{K} = \mathbb{I}$, $\nu = 0.0001$, $g = S = 1$, and
 196 $\gamma_f = \gamma_p = 0$. The figure shows that for this choice of ν , the time-step constraint
 197 is between $1/15$ and $1/10$ which is more restrictive compared to that for Figure
 198 3 for which $\nu = 1$. Thus, we note that the theoretical time step size constraint
 199 (57) decreases as ν becomes smaller so that the long-time numerical results of
 200 Figures 3 and 4 are consistent with our long-time stability analysis.

201 For Figure 5, we set $h = 1/128$, $\mathbb{K} = 0.01\mathbb{I}$, $\nu = g = S = 1$, and $\gamma_f = \gamma_p = 0$.
 202 The figure shows that for this choice of \mathbb{K} , the time-step constraint is between

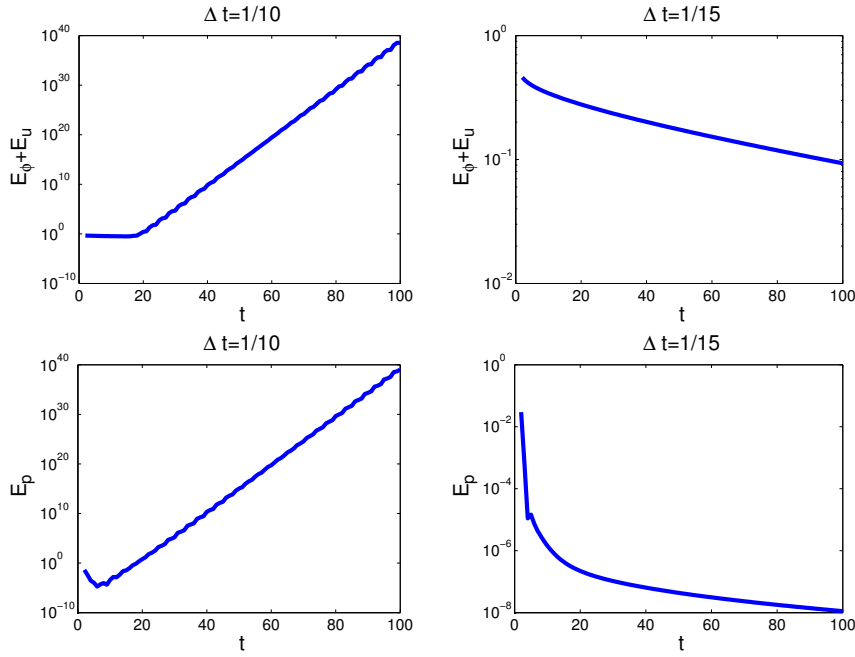


Fig. 4 Long-time behavior of the functionals $E_\phi + E_u$ (top row) and E_p (bottom row) for $\nu = 0.0001$ and $\mathbb{K} = \mathbb{I}$.

203 1/50 and 1/45 which is more restrictive compared to that for Figure 3 for
 204 which $\mathbb{K} = \mathbb{I}$. Thus, again, the long-time numerical results of Figures 3 and
 205 5 are consistent with the theoretical time-step size constraint (57), i.e., the
 206 time-step constraint becomes smaller as the minimum eigenvalue of \mathbb{K} becomes
 207 smaller.

208 For Figure 6, we set $h = 1/128$, $\mathbb{K} = 0.01I$, $\nu = g = S = 1$, and $\gamma_f =$
 209 $\gamma_p = g/2$. The figure shows that for this choice of γ_f and γ_p , the time-step
 210 constraint is between 1/45 and 1/40 which is less restrictive compared to that
 211 for Figure 5 for which $\gamma_f = \gamma_p = 0$. Thus the results show that the stabilizing
 212 term does provide better long-time stability.

213 5 Concluding remarks

214 We proposed and investigated a long-time, third-order accurate, and effi-
 215 cient numerical method for coupled Stokes-Darcy systems. The algorithm is
 216 a combination of a novel third-order Adams-Moulton method and a Adams-
 217 Bashforth method. Our algorithm is a special case of the class of implicit-
 218 explicit (IMEX) schemes. The interfacial term that requires communications
 219 between the porous media and conduit, i.e., between the Stokes and Darcy
 220 components of the model, is treated explicitly in our scheme so that, at each
 221 time step, only two decoupled problems (one Stokes and one Darcy) are solved.

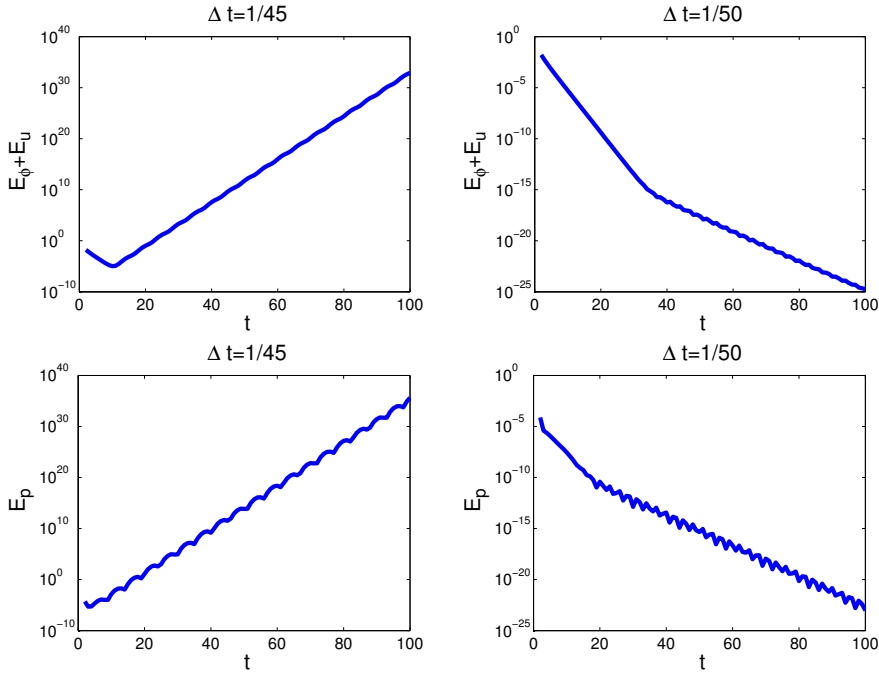


Fig. 5 Long-time behavior of the functionals $E_\phi + E_u$ (top row) and E_p (bottom row) for $\nu = 1$ and $\mathbb{K} = 0.011$.

222 Therefore, our scheme can be implemented very efficiently and, in particular,
 223 legacy codes can be used for each component.

224 We have shown that our scheme is unconditionally stable and, with a
 225 mild time-step restriction, long-time stable in the sense that solutions remain
 226 bounded uniformly in time. The uniform bound in time of the solution leads
 227 to uniform in time error estimates. This is a highly desirable feature because
 228 the physically interesting phenomena of contaminant sequestration and re-
 229 lease usually occur over a very long time scale and one would like to have
 230 faithful numerical results over such time scales. The estimates are illustrated
 231 by numerical examples. All these features suggest that the method has strong
 232 potential in real applications.

233 Methods having even higher-order temporal accuracy and the desired un-
 234 conditional and long-time stability can be derived via suitable combination of
 235 a higher-order Adams-Moulton method for the dissipative term and a stan-
 236 dard Adams-Bashforth method for the interface term. Details will be reported
 237 on elsewhere.

238 References

- 239 1. G. AKRIVIS, M. CROUZEIX, AND C. MAKRIDAKIS, *Implicit-explicit multistep finite element*
 240 *methods for nonlinear parabolic problems*, Math. Comp, 67 (1998), pp. 457-477.

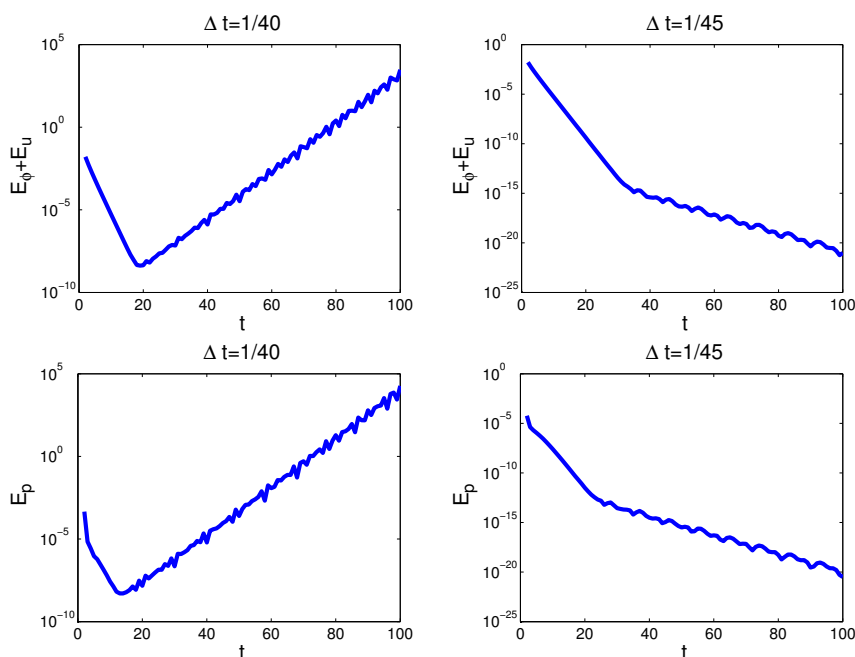


Fig. 6 Long-time behavior of the functionals $E_\phi + E_u$ (top row) and E_p (bottom row) for $\nu = 1$, $\mathbb{K} = 0.01\mathbb{I}$, and $\gamma_f = \gamma_p = g/2$.

- 241 2. G. AKRIVIS, M. CROUZEIX, AND C. MAKRIDAKIS, *Implicit-explicit multistep methods for*
242 *quasilinear parabolic equations*, Numer. Math., 82 (1999), pp. 521-541.
- 243 3. G. AKRIVIS AND Y. SMYRLIS, *Implicit-explicit BDF methods for the Kuramoto-*
244 *Sivashinsky equation*, Appl. Numer. Math., 51 (2004), pp. 151-169.
- 245 4. M. ANITESCU, F. PAHLEVANI, AND W. LAYTON, *Implicit for local effects and explicit*
246 *for nonlocal effects is unconditionally stable*, Electron. Trans. Numer. Anal., 18 (2004),
247 pp. 174-187.
- 248 5. U. ASCHER, S. RUUTH, AND B. WETTON, *Implicit-explicit methods for time-dependent*
249 *partial differential equations*, SIAM J. Numer. Anal., 32 (1995), pp. 797-823.
- 250 6. G. BEAVERS AND D. JOSEPH, *Boundary conditions at a naturally permeable wall*, J. Fluid
251 Mech., 30 (1967), pp. 197-207.
- 252 7. Y. BOUBENDIR AND S. TLUPOVA, *Domain Decomposition Methods for Solving Stokes-*
253 *Darcy Problems with Boundary Integrals*, SIAM J. Sci. Comput., 35(1) (2013), pp. B82-
254 B106.
- 255 8. Y. CAO, M. GUNZBURGER, F. HUA, AND X. WANG, *Coupled Stokes-Darcy Model with*
256 *Beavers-Joseph Interface Boundary Condition*, Comm. Math. Sci., 8 (2010), pp. 1-25.
- 257 9. Y. CAO, M. GUNZBURGER, B. HU, F. HUA, X. WANG, AND W. ZHAO, *Finite element ap-*
258 *proximation of the Stokes-Darcy flow with Beavers-Joseph interface boundary condition*,
259 SIAM J. Num. Anal., 47 (2010), pp. 4239-4256.
- 260 10. Y. CAO, M. GUNZBURGER, X. HE AND X. WANG, *Robin-Robin Domain decomposition*
261 *method for Stokes-Darcy model with Beaver-Joseph interface condition*, Numer. Math.,
262 117 (2011), pp. 601-629.
- 263 11. Y. CAO, M. GUNZBURGER, X. HE AND X. WANG, *Parallel, non-iterative, multi-physics*
264 *domain decomposition methods for time-dependent Stokes-Darcy systems*, Math. Comp.,
265 S 0025-5718 (2014) 02779-8.
- 266 12. A. CEMELIOGLU, V. GIRAULT AND B. RIVIERE. *Time-dependent coupling of Navier-*
267 *Stokes and Darcy flows*, ESAIM Math. Model. Numer. Anal., doi:10.1051/m2an/2012034.

- 268 13. J. CHEN, S. SUN AND X.P. WANG, *A numerical method for a model of two-phase flow*
269 *in a coupled free flow and porous media system*, J Comput. Phys., 268(2014), pp. 1-16.
- 270 14. W. CHEN, P. CHEN, M. GUNZBURGER AND N. YAN, *Superconvergence analysis of FEMs*
271 *for the Stokes-Darcy System*, Math. Meth. the Appl. Sci., 33 (2010), pp. 1605-1617.
- 272 15. W. CHEN, M. GUNZBURGER, F. HUA, AND X. WANG, *A parallel Robin-Robin domain*
273 *decomposition method for the Stokes-Darcy system*, SIAM J. Numer. Anal., 49 (2011),
274 pp. 1064-1084.
- 275 16. W. CHEN, M. GUNZBURGER, D. SUN, AND X. WANG, *Efficient and long-time accurate*
276 *second order methods for Stokes-Darcy system*, SIAM Journal of Numerical Analysis,
277 51(5)2013, pp. 2563-2584.
- 278 17. P. CIARLET, *The Finite Element Method for Elliptic Problems*, North-Holland, Amster-
279 dam, 1978.
- 280 18. M. DISCACCIATI, E. MIGLIO, AND A. QUARTERONI, *Mathematical and numerical models*
281 *for coupling surface and groundwater flows*, Appl. Num. Math., 43 (2002), pp. 57-74.
- 282 19. M. DISCACCIATI AND A. QUARTERONI, *Analysis of a domain decomposition method for*
283 *the coupling of Stokes and Darcy equations*, In Numerical Mathematics and Advanced
284 Applications-ENUMATH 2001, F. Brezzi et al., eds, pp. 3-20, Springer-Verlag, Milan,
285 2003.
- 286 20. M. DISCACCIATI, A. QUARTERONI, AND A. VALLI, *Robin-Robin domain decomposition*
287 *methods for the Stokes-Darcy coupling*, SIAM J. Num. Anal., 45 (2007), pp. 1246-1268.
- 288 21. M. DISCACCIATI AND A. QUARTERONI, *Navier-Stokes/Darcy coupling: modeling, analy-*
289 *sis and numerical approximation*, Rev. Mat. Complut., 22(2) (2009), pp. 315-426.
- 290 22. V.J. ERVIN, E.W. JENKINS AND H. LEE, *Approximation of the Stokes-Darcy system by*
291 *optimization*, J. Sci. Comput., 59(3) (2014), pp. 775-794.
- 292 23. W. FENG, X. HE, Z. WANG AND X. ZHANG, *Non-iterative domain decomposition meth-*
293 *ods for a non-stationary Stokes-Darcy model with Beavers-Joseph interface condition*,
294 Appl. Math. Comput., 219(2) (2012), pp. 453-463.
- 295 24. J. FRANK, W. HUNSDORFER, AND J. VERWER, *Stability of implicit-explicit linear mul-*
296 *tistep methods*, Appl. Numer. Math., 25 (1996), pp. 193-205.
- 297 25. J. GALVIS AND M. SARKIS, *Non-matching mortar discretization analysis for the coupling*
298 *Stokes-Darcy equations*, Electron. Trans. Numer. Anal., 26 (2007), pp. 350-384.
- 299 26. V. GIHAULT AND P.A. RAVIART, *Finite Element Methods for Navier-Stokes Equations:*
300 *Theory and Algorithms*, Springer-Verlag, Berlin, 1986
- 301 27. R. GLOWINSKI, T. PAN, AND J. PERIAUX, *A Lagrange multiplier/fictitious domain*
302 *method for the numerical simulation of incompressible viscous flow around moving grid*
303 *bodies: I. Case where the rigid body motions are known a priori*, C. R. Acad. Sci. Paris
304 Sèr. I Math., 324 (1997), pp. 361-369.
- 305 28. E. HAIRER AND G. WANNER, *Solving Ordinary Differential Equations II: Stiff and*
306 *Differential-Algebraic Problems* 2nd ed, Springer-Verlag, Berlin, 2002.
- 307 29. A. HILL AND E. SÜLLI, *Approximation of the global attractor for the incompressible*
308 *Navier-Stokes equations*, IMA J. Num. Anal., 20 (2000), pp. 633-667.
- 309 30. W. JÄGER AND A. MIKELIĆ, *On the interface boundary condition of Beavers, Joseph*
310 *and Saffman*, SIAM J. Appl. Math., 60 (2000), pp. 1111-1127.
- 311 31. I. JONES, *Low Reynolds number flow past a porous spherical shell*, Proc. Camb. Phil.
312 Soc., 73 (1973), pp. 231-238.
- 313 32. T. KINCAID, *Exploring the Secrets of Wakulla Springs*, Open Seminar, Tallahassee,
314 2004.
- 315 33. M. KUBACKI, *Uncoupling Evolutionary Groundwater-Surface Water Flows Using the*
316 *Crank-Nicolson Leapfrog Method*, Numer. Methods Partial Differential Eq., 29(4) (2013),
317 pp. 1192-1216.
- 318 34. E. KUNIANSKY, *U.S. Geological Survey Karst Interest Group Proceedings*, U.S. Geolog-
319 ical Survey Scientific Investigations Report, Bowling Green, pp. 2008-5023, 2008.
- 320 35. W. LAYTON, F. SCHIEWECK, AND I. YOTOV, *Coupling fluid flow with porous media flow*,
321 SIAM J. Num. Anal., 40 (2003), pp. 2195-2218.
- 322 36. W. LAYTON, H. TRAN, AND C. TRENCHIA, *Analysis of long time stability and errors*
323 *of two partitioned methods for uncoupling evolutionary groundwater-surface water flows*,
324 SIAM J. Numer. Anal., 51(1) (2013), pp. 248-272.

- 325 37. W. LAYTON, H. TRAN AND X. XIONG, *Long time stability of four methods for splitting*
326 *the evolutionary Stokes-Darcy problem into Stokes and Darcy subproblems*, J. Comput.
327 Appl. Math., 236 (2012), pp. 3198-3217.
- 328 38. W.J. LAYTON AND C. TRENCHIA, *Stability of two IMEX methods, CNLF and BDF2-*
329 *AB2, for uncoupling systems of evolution equations*, Appl. Numer. Math., 62 (2012),
330 pp. 112-120.
- 331 39. H. LEE AND K. RIFE, *Least squares approach for the time-dependent nonlinear Stokes-*
332 *Darcy flow*, Math. Method Appl. Sci., 67(10) (2014), pp. 1806-1815.
- 333 40. A. MÁRQUEZ, S. MEDDAHI AND F.J. SAYAS, *A decoupled preconditioning technique for*
334 *a mixed Stokes-Darcy model*, J. Sci. Comput., 57(1) (2013), pp. 174-192.
- 335 41. M. MU AND J. XU, *A two-grid method of a mixed Stokes-Darcy model for coupling fluid*
336 *flow with porous media flow*, SIAM J. Numer. Anal., 45 (2007), pp. 1801-1813.
- 337 42. M. MU AND X. ZHU, *Decoupled schemes for a non-stationary mixed Stokes-Darcy model*,
338 *Math. Comp.*, 79 (2010), pp. 707-731.
- 339 43. A. QUARTERONI AND A. VALLI, *Domain Decomposition Methods for Partial Differential*
340 *Equations*, Oxford Science Publications, Oxford, 1999.
- 341 44. P. SAFFMAN, *On the boundary condition at the interface of a porous medium*, Stud. in
342 Appl. Math., 1 (1971), pp. 77-84.
- 343 45. L. SHAN, H. ZHENG, AND W. LAYTON, *A decoupling method with different subdomain*
344 *time steps for the nonstationary Stokes-Darcy model*, Numer. Meth. Part. D. E., 29(2)
345 (2013), pp. 549-583.
- 346 46. L. SHAN AND H. ZHENG, *Partitioned Time Stepping Method for Fully Evolutionary*
347 *Stokes-Darcy Flow with Beavers-Joseph Interface Conditions*, SIAM J. Numer. Anal.,
348 51(2) (2013), pp. 813-839.
- 349 47. Z. SI, Y. WANG AND S. LI, *Decoupled modified characteristics finite element method for*
350 *the time dependent Navier-Stokes/Darcy problem*, Math. Method Appl. Sci., 37(9) (2014),
351 pp. 1392-1404.
- 352 48. L. ZUO AND Y. HOU, *A decoupling two-grid algorithm for the mixed Stokes-Darcy model*
353 *with the Beavers-Joseph interface condition*, Numer. Meth. Part. D. E., 30(3) (2014),
354 pp. 1066-1082.